4216 *J. Chem. Eng. Data* **2010,** *55,* 4216–4220

Metastable Phase Equilibrium in the Aqueous Quaternary System ($NaCl + MgCl_2 + Na_2SO_4 + MgSO_4 + H_2O$) at 323.15 K[†]

Yafei Guo,[‡,§] Hongjun Yin,[‡,⊥] Xianghua Wu,[‡,⊥] and Tianlong Deng*[,‡,§,||]

College of Materials, Chemistry and Chemical Engineering, Chengdu University of Technology, Chengdu 610059, P. R. China, Tianjin Key Laboratory of Marine Resources and Chemistry, College of Marine Science and Engineering, Tianjin University of Science and Technology, Tianjin 300457, P. R. China, ACS Key Laboratory of Salt Lake Resources and Chemistry, Qinghai Institute of Salt Lakes at Chinese Academy Sciences, Xining 810008, P. R. China, and Institute of Petroleum Geochemical Exploration, Exploration and Production Research Institute, SINOPEC, Hefei 230022, P. R. China

Experimental studies on the metastable solubilities and physicochemical properties (density, viscosity, pH, and refractive index) of the aqueous quaternary system ($NaCl + MgCl_2 + Na_2SO_4 + MgSO_4 + H_2O$) at 323.15 K were determined with the method of isothermal evaporation. On the basis of experimental data, the metastable phase diagram and the diagram of physicochemical properties versus composition were plotted. There are six invariant points, twelve univariant curves, and seven crystallization zones corresponding to halite, thenardite, vanthoffite ($3NaSO_4 \cdot MgSO_4$), astrakanite ($NaSO_4 \cdot MgSO_4 \cdot 4H_2O$), hexahydrite ($MgSO_4 \cdot 6H_2O$), tetrahydrite ($MgSO_4 \cdot 4H_2O$), and bischofite ($MgCl_2 \cdot 6H_2O$). There is no solid solution except two double salts of vanthoffite and astrakanite which existed in the metastable system. When compared with the stable equilibrium phase diagram at 328.15 K, the crystallized zones of loeweite ($6Na_2SO_4 \cdot 7MgSO_4 \cdot 15H_2O$) and kieserite ($MgSO_4 \cdot H_2O$) disappeared; the areas of halite and hexahydrite increased; and the areas of thenardite, astrakanite, and vanthoffite decreased. It is indicated that the metastable phenomena of sodium sulfate and magnesium sulfate are significant. The physicochemical properties (density, viscosity, pH, and refractive index) in the metastable equilibrium system change regularly with the mass fraction change of the magnesium ion.

Introduction

There are more than 700 salt lakes, each with an area larger than 1 km^2, in the Qinghai-Tibet Plateau, China. Salt Lakes of the Qaidam Basin consist of a series of lakes including Caerhan Lake, Dongtai Lake, Xitai Lake, and Yiliping Lake and are a subtype of magnesium sulfate brines famous for their abundance of lithium, potassium, magnesium, and boron resources. The brines mostly belong to the complex seven-component system of ($Li + Na + K + Mg + Cl + SO_4 + B_4O_7 + H_2O$). The phenomena of supersaturation of brines containing magnesium sulfate are often found both in salt lakes and in solar ponds.[1] To economically exploit the brine and mineral resources, it is important to adequately adopt local natural resources such as wind energy and solar energy. Therefore, simulative experimental studies on metastable phase equilibria are essential to predict the path of mineral crystallization for the effective separation and purification of the mixture salts.

Although metastable equilibria for the systems ($KCl + K_2SO_4 + K_2B_4O_7 + H_2O$) and ($NaCl + KCl + Na_2B_4O_7 + K_2B_4O_7 + H_2O$) at 308.15 K, ($NaCl + KCl + CaCl_2 + H_2O$) at 288.15 K, and ($KCl + CaCl_2 + H_2O$) and ($Li_2SO_4 + MgSO_4 + H_2O$) at (288.15, 308.15, and 348.15) K and the stable equilibrium for ($Li_2SO_4 + MgSO_4 + H_2O$) at 348.15 K have been reported,[2−8] the metastable phase equilibrium on the quaternary system ($NaCl + MgCl_2 + Na_2SO_4 + MgSO_4 + H_2O$) at 323.15 K is not reported in the literature. In this paper, the metastable solubilities and the solution physicochemical properties (densities and refractive index) of the quaternary system ($NaCl + MgCl_2 + Na_2SO_4 + MgSO_4 + H_2O$) at 323.15 K are presented.

Experimental Section

Apparatus and Reagents. The isothermal evaporation box was made in our laboratory. In an air-conditioned laboratory, a thermal insulation material box (70 cm long, 65 cm wide, 60 cm high) with an electric fan was installed with an apparatus to control the temperature, which includes three parts: an electric relay, an electrical contact thermograph, and heating lamps (incandescent and ultrared bulbs) as shown in Figure 1. Therefore, the temperature in the box could always be kept within (323.15 ± 0.2) K. An electric fan installed on the box always worked to accelerate the evaporation of water from the solutions. The solid phase minerals were identified with an XP-300 Digital Polarizing Microscope (Shanghai Caikon Optical Instrument Co. Ltd., China) and an X-ray diffractometer (X'pert PRO, Spectris. Pty. Ltd., The Netherlands).

The chemicals used were of analytical grade and obtained from either the Tianjin Kermel Chemical Reagent Ltd. or the Shanghai-Lithium Industrial Co. Ltd., sodium chloride (NaCl, $w = 0.995$ in mass fraction), bischofite ($MgCl_2 \cdot 6H_2O$, $w = 0.995$), sodium sulfate anhydrate (Na_2SO_4, $w = 0.995$), and epsomite ($MgSO_4 \cdot 7H_2O$, $w = 0.990$), and were recrystallized with doubly deionized water (DDW) before use. DDW with a conductivity less than $1 \cdot 10^{-4}$ $S \cdot m^{-1}$ at room temperature (298.15 K) was used to prepare the series of artificially synthesized brines and for chemical analysis.

[†] Part of the "Sir John S. Rowlinson Festschrift".

* Corresponding author. E-mail: tldeng@tust.edu.cn. Tel. & Fax: +86-22-60602962.

[‡] Chengdu University of Technology.

[§] Tianjin University of Science and Technology.

[||] Qinghai Institute of Salt Lakes at Chinese Academy Sciences.

[⊥] Exploration and Production Research Institute.

10.1021/je100365c

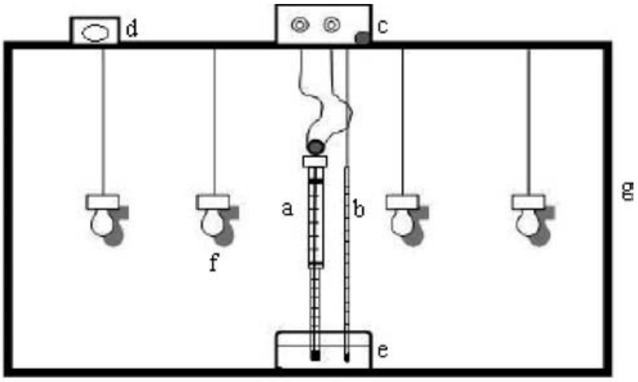

Figure 1. Schematic diagram of the isothermal evaporation chamber. a, electrical contact thermograph; b, precise thermometer; c, electric relay; d, electric fan; e, evaporating container; f, heating lamp; g, isothermal container.

Experimental Methods. The isothermal evaporation method was used in this study. According to phase equilibrium composition, the appropriate quantity of salts and DDW was mixed together as a series of artificially synthesized brines and loaded into clean polyethylene containers (15 cm in diameter, 6 cm high), which were put into the box for isothermal evaporation at (323.15 ± 0.2) K. The experimental conditions of an air flow velocity of (3.5 to 4.0) $\mathrm{m \cdot s^{-1}}$, a relative humidity of (20 to 30) %, and an evaporation rate of (4 to 6) $\mathrm{mm \cdot day^{-1}}$ are similar to those of the climate of the Qaidam Basin. The solutions were not stirred for metastable evaporation, and the crystal behavior of the solid phase was observed periodically. When enough new solid phases appeared (about (0.5 to 1.0) g), the wet residue mixtures were taken out from the solution. The solids were then evaluated with combined chemical analysis, observed with XP-300D Digital Polarizing Microscopy, and further identified with X-ray diffraction. Meanwhile, a 5.0 mL sample of the clear liquid phase solution was taken out from the liquid phase of each polyethylene container through a pipet and then diluted to 250.0 mL in a volumetric flask with DDW for the quantitative analysis of the compositions of the liquid phase. Another aliquot of the clear liquid phase solution was used to measure the relative physicochemical properties individually. The remainder of the solution continued to be evaporated and reached a new metastable equilibrium point.

Analytical Methods. The concentration of SO_4^{2-} in the liquid phase was analyzed by a gravimetric method using barium chloride with a precision within ± 0.05 %. Both with a precision within ± 0.3 %, the concentrations of chloride ion and magnesium ion in the liquids were determined by titration with mercury nitrate standard solution in the presence of mixed indicator of diphenylcarbazone and bromphenol blue and with

Table 1. Metastable Equilibrium Solubilities of the Quaternary System ($NaCl + MgCl_2 + Na_2SO_4 + MgSO_4 + H_2O$) at 323.15 K

	composition of liquid phase w/%				composition of dried salt J, (mol/100 mol dried salt)			
no.	Mg^{2+}	Na^{+}	Cl^{-}	SO_4^{2-}	Na_2^{2+}	SO_4^{2-}	H_2O	solid phase[a]
1,A	0.00	11.43	14.20	1.55	100.0	19.46	1557	H + Th
2	0.47	10.63	13.96	1.73	92.22	21.52	1543	H + Th
3	1.21	9.65	13.15	2.38	80.81	28.60	1472	H + Th
4	1.68	11.39	15.77	3.02	78.20	29.77	1460	H + Th
5	1.76	8.98	12.63	2.87	73.01	33.41	1411	H + Th
6	1.89	8.77	12.53	2.94	71.03	34.17	1405	H + Th
7,E_1	2.03	8.77	12.06	3.34	69.58	37.98	1359	H + Th + Van
8	2.07	8.75	12.06	3.37	69.16	38.12	1353	Th + Van
9	2.17	8.56	10.21	4.23	67.51	47.79	1336	Th + Van
10,E_2	2.46	8.33	8.34	5.28	64.40	58.56	1279	Th + Van + Ast
11	2.45	7.96	5.99	6.07	63.19	69.14	1325	Th + Ast
12	2.91	7.79	2.82	8.00	58.61	86.26	1199	Th + Ast
13,B	3.37	7.15	0.00	9.43	47.17	100.0	1155	Th + Ast
14	1.94	8.73	12.48	3.00	70.42	34.74	1397	H + Van
15	2.53	7.77	12.62	3.05	61.85	34.83	1381	H + Van
16,E_3	2.58	7.57	12.82	2.89	60.81	33.23	1402	H + Van + Ast
17	3.11	6.46	13.61	2.46	52.30	28.55	1435	H + Ast
18	3.79	5.55	13.54	2.75	43.62	31.01	1381	H + Ast
19	5.46	4.48	15.06	3.52	30.27	34.05	1111	H + Ast
20	5.66	3.18	13.48	3.59	22.90	37.09	1229	H + Ast
21	6.00	2.64	13.16	3.80	18.89	38.97	1219	H + Ast
22,E_4	6.33	2.47	13.12	4.14	17.07	41.11	1161	H + Ast + Hex
23	6.44	2.51	12.58	4.55	17.08	44.43	1127	Ast + Hex
24	6.23	2.58	11.48	4.82	17.95	48.16	1160	Ast + Hex
25	5.93	2.86	7.62	6.37	20.30	64.86	1170	Ast + Hex
26	5.99	2.68	2.73	8.53	19.12	87.33	1149	Ast + Hex
27	5.98	2.65	2.43	8.64	18.95	88.71	1152	Ast + Hex
28,C	6.06	2.57	0.00	9.78	18.33	0.00	1129	Ast + Hex
29	6.66	2.12	13.70	4.06	14.38	39.61	1134	H + Hex
30	6.83	2.01	14.14	4.03	13.44	38.64	1109	H + Hex
31	7.31	1.32	16.05	3.31	8.74	31.34	1101	H + Hex
32,E_5	7.57	0.99	16.87	3.04	6.56	28.51	1091	H + Hex + Tet
33	7.97	0.33	17.76	2.72	2.12	25.28	1089	H + Tet
34	8.71	0.32	20.54	2.42	1.93	20.68	960	H + Tet
35	8.56	0.33	21.28	1.90	1.97	16.51	990	H + Tet
36,E_6	9.70	0.12	26.17	1.05	0.65	8.15	841	H + Tet + Bis
37	9.67	0.053	26.55	0.79	0.29	6.17	854	H + Bis
38,F	9.45	0.059	27.65	0.00	0.33	0.00	894	H + Bis
39,D	8.56	0.00	19.62	7.26	0.00	30.83	-	Hex + Tet
40,E	9.65	0.00	26.06	2.87	0.00	8.14	-	Tet + Bis

[a] H, NaCl; Th, Na_2SO_4; Van, $NaSO_4 \cdot 3MgSO_4$; Ast, $NaSO_4 \cdot MgSO_4 \cdot 4H_2O$; Hex, $MgSO_4 \cdot 6H_2O$; Tet, $MgSO_4 \cdot 4H_2O$; Bis, $MgCl_2 \cdot 6H_2O$.

Table 2. Physicochemical Property Data for the Metastable Quaternary System ($NaCl + MgCl_2 + Na_2SO_4 + MgSO_4 + H_2O$) at 323.15 K

		refractive index	viscosity $10^{-3}\eta$	density ρ
no.	pH	n_D	pa·s	$g \cdot cm^{-3}$
1,A	7.11	1.3812	1.0671	1.2228
2	6.65	1.3820	1.1750	1.2373
3	6.50	1.3865	1.3544	1.2561
4	6.58	1.3870	1.3912	1.2591
5	—	1.3900	1.7350	1.2711
6	—	1.3902	1.7659	1.2722
7,E_1	7.27	1.3918	1.8748	1.2853
8	7.27	1.3918	1.8748	1.2853
9	7.29	1.3930	1.4658	1.3017
10,E_2	7.40	1.3950	1.6630	1.3252
11	6.93	1.3930	2.0568	1.3321
12	6.78	1.3956	3.7225	1.3870
13,B	4.41	1.3970	4.7953	1.4190
14	4.41	1.3910	1.5469	1.2735
15	7.28	1.3932	1.8919	1.2778
16,E_3	6.25	1.3936	1.6403	1.2720
17	6.48	1.3925	1.7129	1.2649
18	6.83	1.3965	1.8672	1.2756
19	5.98	1.4005	2.6374	1.2945
20	5.20	1.4040	2.8493	1.3119
21	5.70	1.4060	3.1976	1.3207
22,E_4	5.70	1.4090	3.5210	1.3315
23	5.25	1.4092	4.0190	1.3445
24	5.46	1.4075	3.7515	1.3403
25	5.62	1.4062	4.2127	1.3686
26	5.70	1.4038	5.9968	1.4135
27	5.60	1.4040	6.1180	1.4180
28,C	3.59	1.4048	8.8757	1.4349
29	4.30	1.4102	3.9688	1.3412
30	4.80	1.4120	3.7498	1.3415
31	5.15	1.4142	4.0918	1.3356
32,E_5	3.80	1.4160	4.2630	1.3355
33	5.05	1.4170	4.5592	1.3164
34	4.35	1.4268	—	1.3444
35	4.21	1.4249	5.2667	—
36,E_6	3.90	1.4378	9.2772	1.3626
37	4.06	1.4368	7.0851	1.3556
38,F	4.28	1.4335	5.9519	1.3596
39,D	3.82	1.4378	7.7800	1.3763
40,E	3.65	1.4368	6.7583	1.3659

standard EDTA solution in the presence of Eriochrome Black-T as an indicator, respectively.[9] The concentration of the sodium ion was evaluated according to ion balance.

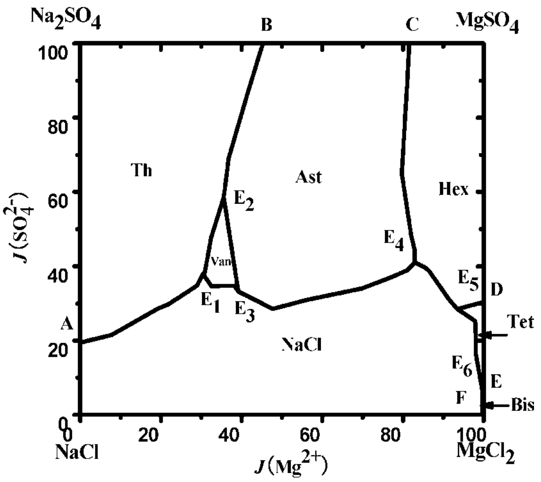

Figure 2. Metastable equilibrium phase diagram of the quaternary system ($NaCl + MgCl_2 + Na_2SO_4 + MgSO_4 + H_2O$) at 323.15 K. Solid line, metastable experimental relationship curve. Th, Na_2SO_4; Van, $NaSO_4 \cdot 3MgSO_4$; Ast, $NaSO_4 \cdot MgSO_4 \cdot 4H_2O$; Hex, $MgSO_4 \cdot 6H_2O$; Tet, $MgSO_4 \cdot 4H_2O$; Bis, $MgCl_2 \cdot 6H_2O$.

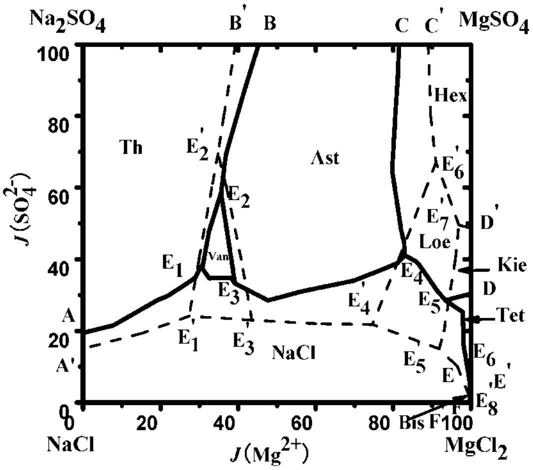

Figure 3. Comparison of the stable phase diagram at 328.15 K[10] and metastable phase diagram at 323.15 K of the quaternary system ($NaCl + MgCl_2 + Na_2SO_4 + MgSO_4 + H_2O$). Solid line, metastable experimental relationship curve; dashed line, stable experimental relationship curve. Th, Na_2SO_4; Van, $NaSO_4 \cdot 3MgSO_4$; Ast, $NaSO_4 \cdot MgSO_4 \cdot 4H_2O$; Loe, $6Na_2SO_4 \cdot 7MgSO_4 \cdot 15H_2O$; Hex, $MgSO_4 \cdot 6H_2O$; Kie, $MgSO_4 \cdot H_2O$; Tet, $MgSO_4 \cdot 4H_2O$; Bis, $MgCl_2 \cdot 6H_2O$.

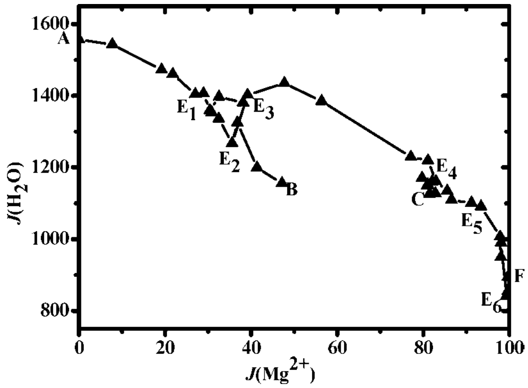

Figure 4. Water-phase diagram of the quaternary system ($NaCl + MgCl_2 + Na_2SO_4 + MgSO_4 + H_2O$) at 323.15 K. ▲, experimental data points; solid line, experimental relationship curves.

A PHS-3C precision pH meter supplied by the Shanghai Precision and Scientific Instrument Co., Ltd. was used to measure the pH of the equilibrium aqueous solutions (precision of ± 0.01). The pH meter was calibrated with two standard buffer solutions of potassium dihydrogen phosphate and disodium hydrogen phosphate (pH 6.98) and borax (pH 9.46). The densities (ρ) were measured with a density bottle $V = 5.0$ mL with a precision of ± 0.2 mg. An Abbe refractometer (model WZS-1) was used to measure the refractive index (n_D), and it was calibrated with the known refractive index of superpure water standard ($n_D = 1.3325$) with a precision of ± 0.0001 (in triplicate measurements). Conductivities (κ) were measured with an Orion 145A+ Conductivity Meter (Thermo Electron Corporation, America) with a precision of $\pm 0.001 \ S \cdot m^{-1}$. All the measurements were maintained at the desired temperature (323.15 ± 0.1) K through control of the thermostat.

Results and Discussion

The metastable solubilities and physicochemical properties of the quaternary system ($NaCl + MgCl_2 + Na_2SO_4 + MgSO_4 + H_2O$) at 323.15 K were determined and are listed in Tables 1 and 2, respectively. On the basis of the Jänecke index (J, J/[mol/100 mol($2Na^+ + Mg^{2+}$)]) in Table 1, the metastable equilibrium phase diagram of the system at 323.15 K was plotted

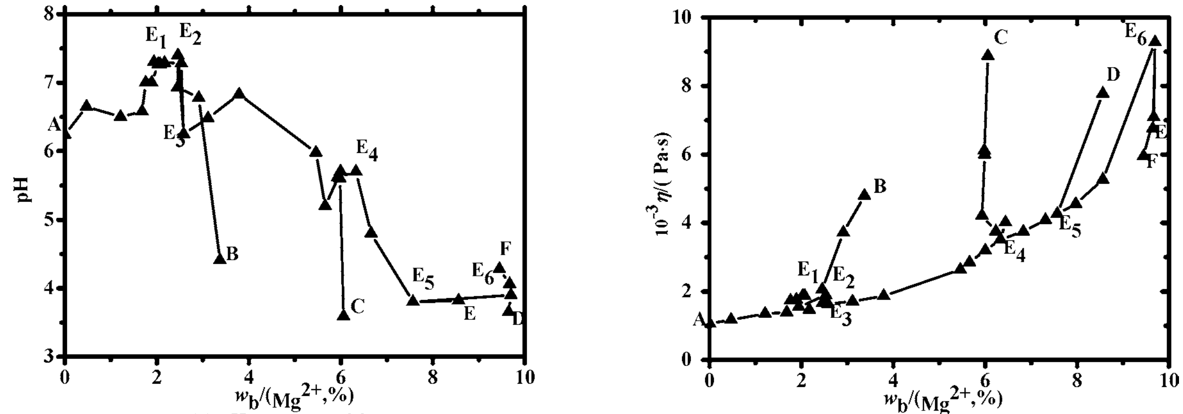

(a) pH vs. composition

(c) Viscosity vs. composition

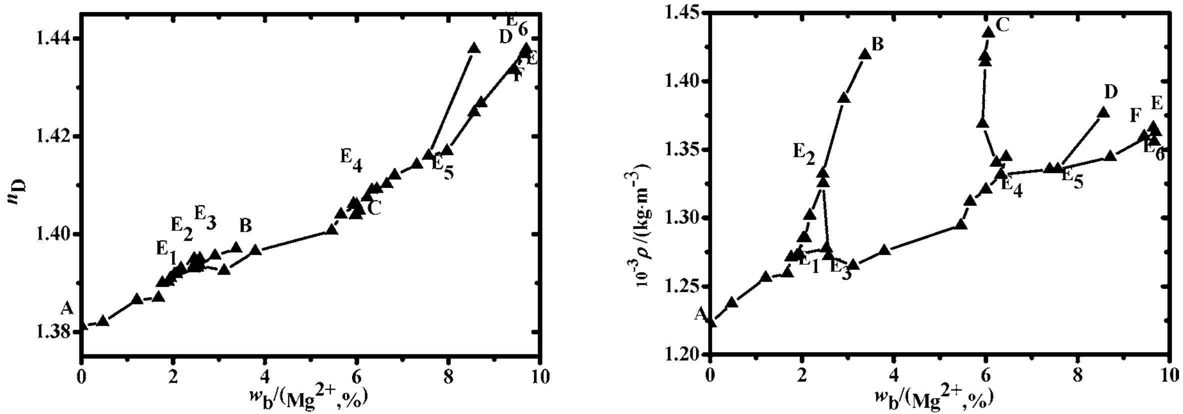

(b) Refractive index vs. composition

(d) Density vs. composition

Figure 5. Physicochemical properties versus composition diagrams for the metastable quaternary system (NaCl + $MgCl_2$ + Na_2SO_4 + $MgSO_4$ + H_2O) at 323.15 K. (a) pH vs composition; (b) refractive index vs composition; (c) viscosity vs composition; and (d) density vs composition. ▲, experimental data points; solid line, experimental relationship curves.

(Figure 2). In Figure 2, the metastable phase diagram consists of six invariant points, twelve univariant curves, and seven crystallization zones corresponding to halite (NaCl), thenardite ($NaSO_4$, Th), vanthoffite ($3NaSO_4\cdot MgSO_4$, Van), astrakanite ($NaSO_4\cdot MgSO_4\cdot 4H_2O$, Ast), hexahydrite ($MgSO_4\cdot 6H_2O$, Hex), tetrahydrite ($MgSO_4\cdot 4H_2O$, Tet), and bischofite ($MgCl_2\cdot 6H_2O$, Bis). It was found that there is no solid solution except for two double salts of vanthoffite and astrakanite that exist in the metastable system. There are no data reported for the stable equilibrium system at 323.15 K; therefore, a comparison of the diagrams of the metastable equilibrium at 323.15 K with solid lines and the stable equilibrium at 328.15 K with dashed lines in the same system is shown in Figure 3. Figure 3 shows that the stable diagram contains eight invariant points. The crystallized zones of loeweite ($6Na_2SO_4\cdot 7MgSO_4\cdot 15H_2O$, Loe) and kieserite ($MgSO_4\cdot H_2O$, Kie) are produced, while the crystallization zones of loeweite and kieserite disappeared. The area of NaCl and hexahydrite ($MgSO_4\cdot 6H_2O$) increased, and the area of thenardite, astrakanite, and vanthoffite decreased in the metastable system. It is indicated that the metastable phenomena of sodium sulfate and magnesium sulfate are significant. Figure 4 is the water-phase diagram of the quaternary system at 323.15 K and shows that the Jänecke index values of $J(H_2O)$ gradually change with increasing $J(Mg^{2+})$.

On the basis of experimental data in Table 2, the relationship of the solution physicochemical properties (densities and refractive index) with the concentration of Mg^{2+} is shown in Figure 5. It can be seen that the solution density, refractive index, and viscosity of the quaternary system gradually increase and the pH value gradually decreases with an increase of the concentration of the magnesium ion.

Conclusions

Metastable equilibrium of the quaternary system (NaCl + $MgCl_2$ + Na_2SO_4 + $MgSO_4$ + H_2O) at 323.15 K was studied with an isothermal evaporation method. Solubilities and the solution physicochemical properties (pH values, viscosities, densities, and refractive index) were determined experimentally. According to the experimental data, the metastable dried-salt phase diagrams, water-phase diagram, and the diagrams of physicochemical properties versus composition were plotted. Those results show that no solid solution is formed. The physicochemical properties including pH, densities, viscosities, and refractive index in the metastable quaternary system change regularly with the mass fraction change of the magnesium ion.

Acknowledgment

Thanks to the Editors and the anonymous reviewers for their critical comments on the manuscript.

Literature Cited

(1) Chen, J. Q.; Liu, Z. Q.; Fang, C. H. Studies on Evaporation-Crystallization of Salt Lake Brines in China. *J. Salt Lake Res.* **1994**, *2*, 43–51.

(2) Deng, T. L.; Wang, S. Q.; Sun, B. Metastable Phase Equilibrium in the Aqueous Quaternary System (KCl + K_2SO_4 + $K_2B_4O_7$ + H_2O) at 308.15 K. *J. Chem. Eng. Data* **2008**, *53*, 411–414.

(3) Deng, T. L.; Meng, L. Z.; Sun, B. Metastable Phase Equilibria of the Reciprocal Quaternary System Containing Sodium, Potassium, Chlorite, and Borate Ions at 308.15 K. *J. Chem. Eng. Data* **2008**, *53*, 704–709.

(4) Deng, T. L.; Li, D. C.; Wang, S. Q. Metastable Phase Equilibrium in the Aqueous Ternary System ($KCl + CaCl_2 + H_2O$) at (288.15 and 308.15) K. *J. Chem. Eng. Data* **2008**, *53*, 1007–1011.

(5) Deng, T. L.; Li, D. C. Solid-liquid Metastable Equilibria in the Quaternary System ($NaCl - KCl - CaCl_2 - H_2O$) at 288.15 K. *Fluid Phase Equilib.* **2008**, *269*, 98–103.

(6) Wang, S. Q.; Deng, T. L. (Solid + liquid) Isothermal Evaporation Phase Equilibria in the Aqueous Ternary System ($Li_2SO_4 + MgSO_4 + H_2O$) at $T = 308.15$ K. *J. Chem. Thermodyn.* **2008**, *40*, 1007–1011.

(7) Deng, T. L.; Yin, H. J.; Li, D. C. Metastable Phase Equilibrium in the Aqueous Ternary System ($Li_2SO_4 + MgSO_4 + H_2O$) at $T = 348.15$ K. *J. Chem. Eng. Data* **2008**, *54*, 498–501.

(8) Lepeshkov, I. N.; Romashova, N. N. The Ternary System Li_2SO_4-$MgSO_4$-H_2O at 75°C. *Russ. J. Inorg. Chem.* **1960**, *5*, 2512−2517.

(9) Qinghai institute of salt lakes of CAS. *Analytical Methods of Brines and Salts*, 2nd ed.; Chin. Sci. Press: Beijing, 1988.

(10) Stephen, H.; Stephen, T. *Solubilities of Inorganic and Organic Compounds*; Parts 1 & 2, Pergamon Press: Oxford, 1963; Vol. 1.

Received for review April 15, 2010. Accepted August 21, 2010. Financial support from the State Key Program of National Natural Science Foundation of China (Grant. 20836009), the National Natural Science Foundation of China (Grant. 40773045), and Senior Professor Program in Tianjin Government for TUST (Grant. 20100405) is greatly acknowledged.

JE100365C